New Journal of Physics
The open-access journal for physics

Route to ponderomotive entanglement of light via optically trapped mirrors

Christopher Wipf[1,3], **Thomas Corbitt**[1], **Yanbei Chen**[2] **and Nergis Mavalvala**[1]

[1] LIGO Laboratory, Massachusetts Institute of Technology, Cambridge, MA 02139, USA
[2] Theoretical Astrophysics, California Institute of Technology, Pasadena, CA 91125, USA
E-mail: wipf@ligo.mit.edu

New Journal of Physics **10** (2008) 095017 (10pp)
Received 13 June 2008
Published 30 September 2008
Online at http://www.njp.org/
doi:10.1088/1367-2630/10/9/095017

Abstract. The radiation pressure of two laser beams detuned from resonance in an optical cavity can create a stable optical trap for a mechanical oscillation mode of a movable cavity mirror. Here it is shown that such a configuration entangles the output light fields via interaction with a mirror that is suspended as a pendulum. The degree of entanglement is quantified spectrally using the logarithmic negativity, and related to the available optical restoring force. Entanglement survives in the experimentally accessible regime of gram-scale masses subject to thermal noise at room temperature.

Contents

[3] Author to whom any correspondence should be addressed.

© IOP Publishing Ltd and Deutsche Physikalische Gesellschaft

Entanglement both provides a basis for fundamental tests of quantum mechanics, and is an ingredient for applications in quantum information, including cryptography and teleportation. Producing entanglement in a macroscopic mechanical system has become a prominent experimental objective, and progress in the fabrication and cooling of small mechanical resonators is quickly bringing this objective within reach [1]–[8], as highlighted in a series of proposals treating these systems. It was predicted that the radiation pressure coupling of light incident on such resonators can entangle them with the optical field [9, 10], or with other resonators [11]–[14], while also allowing the devices to act as sources of entangled light [15, 16]. Analogous effects are possible when capacitive coupling is substituted for the radiation pressure [17]. Recent work carries such predictions to high temperatures, and more experimentally relevant parameter regimes [18]–[20].

Meanwhile, the improving sensitivity of gravitational-wave interferometers is opening a new experimental regime for macroscopic quantum mechanics, and may reveal quantum features, such as squeezing and entanglement of their mirrors' motion [21]. In addition to the profoundly macroscopic size of these systems, a further distinctive feature of this regime is that radiation pressure effects, in particular the optical spring [22]–[26], can play a dominant role in the dynamics.

A demonstrative example is the stable optical trap for macroscopic mirrors, presented in [27]. This technique exploits the radiation pressure of two laser fields detuned from cavity resonance to create simultaneously an optical restoring force and damping force that overwhelm their mechanical counterparts, thereby fixing the mirror in place. When the energy stored in the dissipative mechanical structure supporting the mirror becomes negligible compared with that stored in the optical field, the deleterious coupling with the thermal environment can be substantially diluted [28]. This makes the system a promising candidate to exhibit quantum effects including entanglement.

Motivated by these developments, here we evaluate the prospects for observing entanglement in the trapped-mirror system. We concentrate on the entanglement between output optical fields, i.e. the device's potential as a source of quadrature-entangled light. Since this type of entanglement places the least stringent demands on the state of the mirror, we expect that it will be among the earliest to be demonstrated experimentally. The protocols developed to characterize previous, non-mechanical quadrature entanglers [29]–[31] can be directly applied in this setting.

This paper is organized as follows. In section 1, we briefly review the logarithmic negativity entanglement measure. In section 2, we describe the dynamics of the stable optical trap in some detail, providing a quantum treatment of a cavity mirror coupled to two optical fields based on their Langevin equations, including thermal noise of the mirror coating. This leads to a simple and general formula quantifying the entanglement of the optical fields at the output, presented in section 3. The prospects for experimentally realizing this entanglement are considered in section 4, before concluding with section 5.

1. Entanglement criterion

Entanglement of a bipartite continuous-variable system can be recognized by inspecting its variance matrix for evidence of non-classical correlation. This 4×4 symmetric matrix contains the second-order moments between elements of a vector of observables $\mathbf{u} = [Q_1, P_1, Q_2, P_2]^T$ (i.e. the canonical positions Q_j and momenta P_j of subsystems $j \in \{1, 2\}$), and is defined

as follows:

$$\boldsymbol{V} = \begin{bmatrix} \boldsymbol{V}_{11} & \boldsymbol{V}_{12} \\ \boldsymbol{V}_{12}^T & \boldsymbol{V}_{22} \end{bmatrix}; \quad \boldsymbol{V}_{jk} = \begin{bmatrix} \langle Q_j Q_k \rangle_+ & \langle Q_j P_k \rangle_+ \\ \langle P_j Q_k \rangle_+ & \langle P_j P_k \rangle_+ \end{bmatrix}. \tag{1}$$

Here $\mathbf{u}$ is assumed to have zero mean (the steady-state value $\bar{u}_j$ of each element has been subtracted, leaving only fluctuating terms). The quantity $\langle uv \rangle_+$ denotes the symmetrized average $\langle uv + vu \rangle / 2$.

The Peres–Horodecki entanglement criterion [32], as stated for continuous-variable systems by Simon [33], establishes that the system is entangled whenever the time reversal of one subsystem only (e.g. $P_2 \to -P_2$) would result in a variance matrix that no longer satisfies the uncertainty principle. Stated mathematically, separability constrains the variance matrix by requiring $4 \det \boldsymbol{V} > \Sigma - \frac{1}{4}$, where $\Sigma = \det \boldsymbol{V}_{11} + \det \boldsymbol{V}_{22} - 2 \det \boldsymbol{V}_{12}$. Further, one may define the logarithmic negativity [34] in terms of $\boldsymbol{V}$:

$$E_N = \max \left[0, -\tfrac{1}{2} \ln \left(2\Sigma - 2\sqrt{\Sigma^2 - 4 \det \boldsymbol{V}} \right) \right]. \tag{2}$$

This entanglement measure quantifies the degree to which the Peres–Horodecki criterion has been violated [35]. Note that the preceding statements presume (dimensionless) canonical commutation relations between the elements of $\mathbf{u}$: $[Q_j, P_k] = \mathrm{i}\delta_{jk}$, and $[Q_j, Q_k] = [P_j, P_k] = 0$.

2. Opto-mechanical dynamics

A schematic of a trapped mirror system is shown in figure 1. In each cavity, the motion of the massive input mirrors can be neglected; moreover, the Michelson readout is decoupled from all disturbances common to both cavities, as discussed in section 4. Hence, we can limit our attention to a single mechanical mode: the differential degree of freedom. To compute its second-order moments, we first write down its linearized, Heisenberg-picture equations of motion, which are derived using the quantum Langevin approach (cf [16, 20, 36]). They can be expressed in the succinct form

$$\dot{\mathbf{u}}_{\mathrm{ic}} = \boldsymbol{K} \mathbf{u}_{\mathrm{ic}} + \mathbf{u}_{\mathrm{in}}. \tag{3}$$

This operator equation relates a vector of intra-cavity coordinates, $\mathbf{u}_{\mathrm{ic}} = [q, p, X_1, Y_1, X_2, Y_2]^T$, and a vector of input noises driving the system, $\mathbf{u}_{\mathrm{in}} = [0, F_{\mathrm{th}}, \sqrt{2\gamma_{\mathrm{c}}} X_{\mathrm{in},1}, \sqrt{2\gamma_{\mathrm{c}}} Y_{\mathrm{in},1} + G_1 q_{\mathrm{s}}, \sqrt{2\gamma_{\mathrm{c}}} X_{\mathrm{in},2}, \sqrt{2\gamma_{\mathrm{c}}} Y_{\mathrm{in},2} + G_2 q_{\mathrm{s}}]^T$, which arise from coupling with the environment. Elements of $\mathbf{u}_{\mathrm{ic}}$ include the coordinates q, p of the mirror, and the cavity optical mode quadrature operators defined by $X_j = (a_j^\dagger + a_j)/\sqrt{2}$, $Y_j = \mathrm{i}(a_j^\dagger - a_j)/\sqrt{2}$. Elements of $\mathbf{u}_{\mathrm{in}}$ include a Langevin force F_{th} driving Brownian motion of the mirror, the vacuum noises $X_{\mathrm{in},j}$, $Y_{\mathrm{in},j}$ entering each cavity mode, and a mirror surface displacement q_{s} due to thermal noise of the optical coating layer. The coupling matrix is

$$\boldsymbol{K} = \begin{bmatrix} 0 & 1/m & 0 & 0 & 0 & 0 \\ -m\omega_{\mathrm{m}}^2 & -\gamma_{\mathrm{m}} & \hbar G_1 & 0 & \hbar G_2 & 0 \\ 0 & 0 & -\gamma_{\mathrm{c}} & \Delta_1 & 0 & 0 \\ G_1 & 0 & -\Delta_1 & -\gamma_{\mathrm{c}} & 0 & 0 \\ 0 & 0 & 0 & 0 & -\gamma_{\mathrm{c}} & \Delta_2 \\ G_2 & 0 & 0 & 0 & -\Delta_2 & -\gamma_{\mathrm{c}} \end{bmatrix}. \tag{4}$$

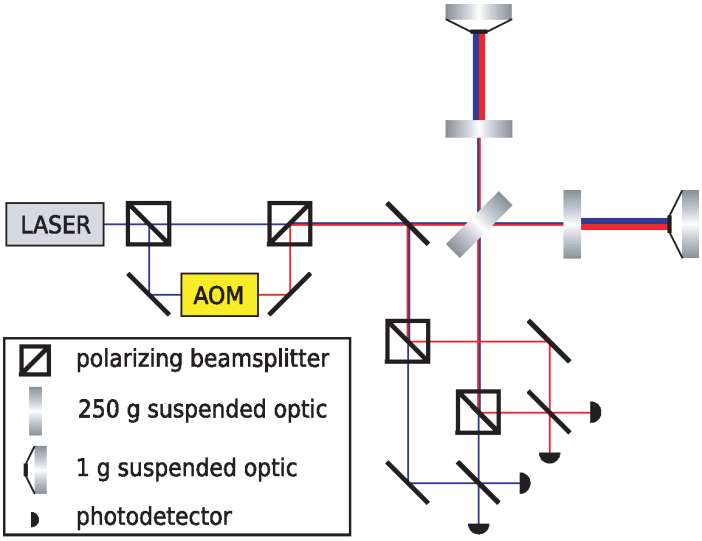

Figure 1. Schematic of an optical trapping and homodyne readout apparatus for the differential mode of a Fabry–Perot Michelson interferometer. Each arm cavity comprises a highly reflective, low-mass end mirror and a massive input mirror of finite transmissivity. The system is driven by two orthogonally polarized laser beams: a strong 'carrier' field, and a weaker frequency-shifted 'subcarrier' created by an acousto-optic modulator (AOM). Each optical field is monitored using a balanced homodyne readout. Feedback loops required to hold the interferometer on resonance are not shown.

Here the cavity mode operators are represented in the frame rotating with their drive fields, so that only their detunings appear in the equations, and $G_j = \alpha_j \omega_c / L$ parametrizes the opto-mechanical coupling. The intra-cavity amplitude near resonance is related to the incident power I_j by $\alpha_j^2 = 4 I_j \gamma_c / [\hbar \omega_c (\gamma_c^2 + \Delta_j^2)]$, and the detuning of each field is $\Delta_j = (1 - \bar{q}/L)\omega_c - \omega_j$. All other parameters are defined in table 1.

Taking the Fourier transform $\mathcal{F}\{f(t)\} = (2\pi)^{-1/2} \int \mathrm{d}t\, f(t) \mathrm{e}^{-\mathrm{i}\Omega t}$, it is straightforward to solve (3) algebraically for $\mathbf{u}_{\mathrm{ic}}$ in terms of $\mathbf{u}_{\mathrm{in}}$ [16]. To gain insight into the solution, we begin with the case where $G_1 = G_2 = 0$, decoupling the subsystems. Then the mirror's equation of motion is that of a thermally driven pendulum, $q(\Omega) = \chi_{\mathrm{m}}(\Omega) F_{\mathrm{th}}(\Omega)$, where the mechanical susceptibility to force is given by $\chi_{\mathrm{m}}(\Omega) = [m(\omega_{\mathrm{m}}^2 + \mathrm{i}\gamma_{\mathrm{m}}\Omega - \Omega^2)]^{-1}$.

Turning on the interaction has two effects on the mirror. Firstly, it introduces new driving terms due to radiation pressure noise. Secondly, it alters the mirror's response function. When motion is slow on the cavity timescale ($\Omega \ll \gamma_c$), the opto-mechanical susceptibility may still be written in the form $\chi_{\mathrm{eff}}(\Omega) = [m(\omega_{\mathrm{eff}}^2 + \mathrm{i}\gamma_{\mathrm{eff}}\Omega - \Omega^2)]^{-1}$, but the system's new resonance parameters are

$$\omega_{\mathrm{eff}}^2 = \omega_{\mathrm{m}}^2 + \sum_j \omega_{\mathrm{eff},j}^2; \quad \omega_{\mathrm{eff},j}^2 = -\frac{\hbar G_j^2 \delta_j}{m(\gamma_c^2 + \Delta_j^2)}, \tag{5}$$

$$\gamma_{\mathrm{eff}} = \gamma_{\mathrm{m}} + \sum_j \gamma_{\mathrm{eff},j}; \quad \gamma_{\mathrm{eff},j} = -\frac{2\gamma_c \omega_{\mathrm{eff},j}^2}{\gamma_c^2 + \Delta_j^2}. \tag{6}$$

In (5), note that $\omega_{\mathrm{eff},j}^2$ takes a negative value whenever Δ_j is positive.

Table 1. Parameters and their nominal values. Note that the optical coating noise parameter C depends on both material and geometric properties of the end mirror, and is broken down further in [37].

Parameter	Symbol	Value
Mirror resonant frequency	$\omega_m/2\pi$	1 Hz
Mirror damping rate	$\gamma_m/2\pi$	1 μHz
Mirror reduced mass	m	0.5 g
Cavity resonant frequency	$\omega_c/2\pi$	$c/(1064\,\text{nm})$
Cavity linewidth (HWHM)	$\gamma_c/2\pi$	9.5 kHz
Cavity length	L	1 m
Carrier power	I_1	5 W
Carrier detuning	Δ_1	$-3\gamma_c$
Subcarrier power	I_2	0.3 W
Subcarrier detuning	Δ_2	$\gamma_c/2$
Coating noise coefficient	C	$1.5\times10^{-13}\,\text{s}^2\,\text{kg}^{-1}$
Ambient temperature	T	300 K

These expressions reveal an important feature of strong radiation pressure coupling: it can create both static and dynamic instability. Considering a *single* optical field j, note that its contributions to the spring constant, $m\omega_{\text{eff},j}^2$, and the damping rate, $\gamma_{\text{eff},j}$, have opposite sign. If both of these terms are permitted to exceed the mechanical contributions, $m\omega_m^2$ and γ_m respectively, then the system becomes unstable. This follows from the presence of either an overall anti-restoring force, or an anti-damping force, depending upon which sign is chosen for the detuning Δ_j. For this reason, prior studies on ponderomotive entanglement have avoided the regime where the optical spring constant dominates. However, in the presence of *two* optical fields, the coupling strengths and detunings can be chosen so that, when considered together, the effective resonant frequency and damping rate both have positive sign, and are dominated by terms of optical origin. These are the conditions needed to realize a stable optical trap [27].

Strong coupling is the prerequisite for optical trapping: strong, in particular, when compared with the mechanical resonant frequency. The optical spring constant is maximized at $\Delta_j = -\gamma_c/\sqrt{3}$, which leads to a criterion

$$\omega_{\text{max},j}^2 \equiv \frac{3\sqrt{3}I_j\omega_c}{4mL^2\gamma_c^2} \gtrsim \omega_m^2 \tag{7}$$

delineating the boundary of the regime where a dominant optical spring is possible.

3. Output variances

The optical fields exiting the cavity are potentially quantum-correlated, due to the coupling of their intra-cavity amplitude and phase with the motion of a common mirror. To study these correlations, the variance matrix of the output fields is obtained from the solution to (3) via the cavity input–output relation, $a_{\text{in}} + a_{\text{out}} = \sqrt{2\gamma_c}a_{\text{ic}}$. First, as $i\Omega$ occurs asymmetrically in the frequency-domain equations, the operators must be made Hermitian by combining the positive and negative frequency parts: $O^{\text{H}}(\Omega) = (O(\Omega) + O(-\Omega))/\sqrt{2}$. Subsequently,

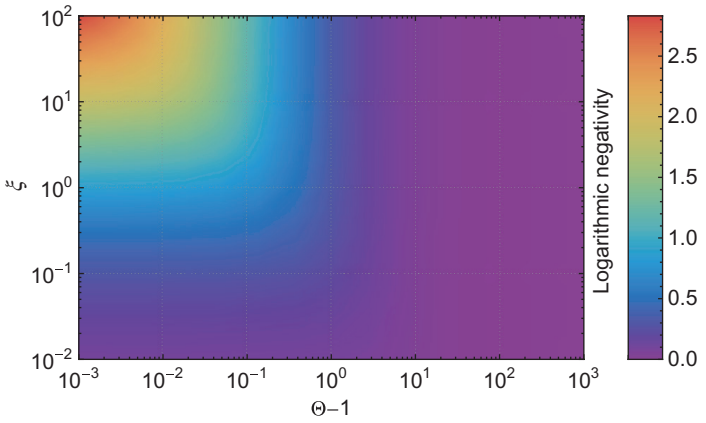

Figure 2. Logarithmic negativity of output carrier–subcarrier entanglement in the dc limit.

one finds the variance matrix of the output spatial mode at sideband frequency Ω, in terms of the correlation spectra of the noise inputs, which are [36, 37]:

$$\langle F_{\rm th}(\Omega)F_{\rm th}(\Omega')\rangle = 2\gamma_{\rm m}m\hbar\Omega N(\Omega)\delta(\Omega+\Omega'), \tag{8}$$

$$\langle a_{{\rm in},j}(\Omega)a^{\dagger}_{{\rm in},k}(\Omega')\rangle = \tfrac{1}{2}\delta_{j,k}\delta(\Omega+\Omega'), \tag{9}$$

$$\langle a_{{\rm in},j}(\Omega)a_{{\rm in},k}(\Omega')\rangle = \langle a^{\dagger}_{{\rm in},j}(\Omega)a^{\dagger}_{{\rm in},k}(\Omega')\rangle = 0, \tag{10}$$

$$\langle q_{\rm s}(\Omega)q_{\rm s}(\Omega')\rangle = \frac{C}{\Omega}k_{\rm B}T\delta(\Omega+\Omega'), \tag{11}$$

with $N(\Omega) = (\mathrm{e}^{\hbar\Omega/k_{\rm B}T}-1)^{-1}$. Moreover, the only non-vanishing commutator among the output fields is $[X^H_{{\rm out},j}(\Omega), Y^H_{{\rm out},j}(\Omega')] = \mathrm{i}\delta(\Omega-\Omega')$.

Applying (2) to these modes, one finds that the logarithmic negativity of the output fields can be written simply in the dc limit ($\Omega \to 0$):

$$e_{N,{\rm out}} = -\tfrac{1}{2}\ln\left(1+2\xi\left[\Theta-\sqrt{\Theta^2+\xi^{-1}}\right]\right), \tag{12}$$

where ξ and Θ are dimensionless quantities parametrizing the entangler strength, and the degradation due to thermal noise, respectively. The dependence of $E_{N,{\rm out}}$ on these quantities is depicted in figure 2. They are defined as

$$\xi = \frac{4\gamma_{\rm c}^2}{\Delta_1\Delta_2}\frac{\omega^2_{{\rm eff},1}\omega^2_{{\rm eff},2}}{\omega^4_{\rm eff}}, \tag{13}$$

$$\Theta = 1+\frac{1}{2}\frac{k_{\rm B}T}{\hbar\omega_{\rm m}Q_{\rm m}}\left(\sum_j \frac{-\omega^2_{\rm m}}{\omega^2_{{\rm eff},j}\gamma_{\rm c}/\Delta_j}\right) \tag{14}$$

using also the mechanical quality factor $Q_{\rm m} = \omega_{\rm m}/\gamma_{\rm m}$. Note that an upper bound for ξ over all detunings is given by

$$\xi \leqslant \frac{1024}{27}\frac{(\omega^2_{{\rm max},1}/\omega^2_{\rm m})(\omega^2_{{\rm max},2}/\omega^2_{\rm m})}{(1+\sum_j \omega^2_{{\rm eff},j}/\omega^2_{\rm m})^2}. \tag{15}$$

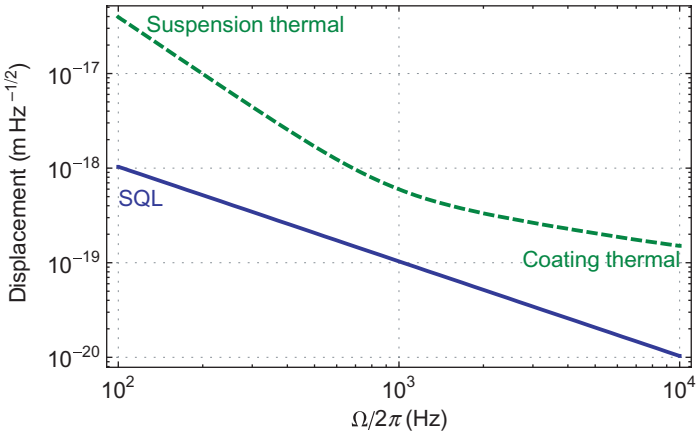

Figure 3. Budget of limiting classical noise sources based on the parameters of table 1, plotted with the standard quantum limit $S_{\mathrm{SQL}}(\Omega) = 2\hbar/(m\Omega^2)$.

Writing ξ in this form makes explicit the connection between a strong entangler and the possibility of a strong optical spring. Unless the criterion (7) is satisfied by at least one field, ξ is constrained to be small.

The expression (14) shows how the entanglement can survive at temperatures that are strikingly high, given the mirror mechanical properties. Here, the factor $k_{\mathrm{B}}T/(\hbar\omega_{\mathrm{m}}Q_{\mathrm{m}})$ can be interpreted as a thermal noise figure of merit for the mechanics; it is, in fact, the limiting thermal occupation number under cold damping. The factor in parentheses represents the optical modification to the mechanical thermal noise. This factor is lower bounded over all detunings by $\sum_j \frac{\sqrt{27}}{16}\omega_{\mathrm{m}}^2/\omega_{\mathrm{max},j}^2$. Hence, when the criterion (7) is satisfied by *both* optical fields, a large suppression of the thermal noise is possible.

4. Experimental prospects

An experiment must contend with technical noise sources such as seismic and laser noise, as well as the noises (vacuum, coating and suspension thermal) that are included in the treatment given here. A more detailed noise study exists for the case where light sensing the motion of two gram-scale mirrors is optically recombined in a Fabry–Perot Michelson interferometer [37]. A schematic description of a proposed experiment is shown in figure 1, and relevant parameter values are summarized in table 1. In such a configuration, the differential motion degree of freedom may be treated as a single cavity wherein common mode laser technical noise largely cancels. In addition, strong restoring and damping forces are supplied to the suspended mirrors by radiation pressure of two detuned optical fields. Consequently the resonant frequency is shifted by three orders of magnitude, from $\omega_{\mathrm{m}}/2\pi = 1\,\mathrm{Hz}$ to $\omega_{\mathrm{eff}}/2\pi \approx 2.3\,\mathrm{kHz}$, with no concomitant increase in the mechanical coupling to the environment. The mirror's response to all external force noises at frequencies well below $\omega_{\mathrm{eff}}/2\pi$ is thereby suppressed by the factor $\omega_{\mathrm{m}}^2/\omega_{\mathrm{eff}}^2$. The combination of noise cancellation and suppression should achieve the classical noise budget presented in figure 3, allowing the prospects for entanglement to be evaluated using the analysis described above.

Results of numerical evaluation of $E_{N,\mathrm{out}}(\Omega)$ are presented in figure 4, showing that entanglement of the output light should be produced within the frequency band of interest,

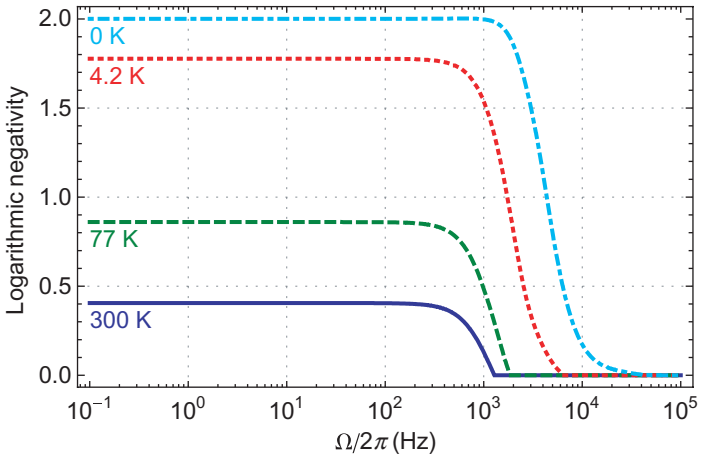

Figure 4. Predicted logarithmic negativity spectra for entanglement of the output carrier and subcarrier fields, plotted for various ambient temperatures T. Additional parameters are specified in table 1.

and that it is remarkably robust against thermal noise—even surviving a room temperature environment. The spectra are flat until suppressed by the onset of the coating noise, with a zero-temperature cutoff at the cavity linewidth $\gamma_c/2\pi \approx 9.5\,\mathrm{kHz}$; the magnitude at low frequency is well approximated by (12).

Given the assumptions of table 1, the entangler strength parameter is $\xi \approx 13.2$, and the thermal degradation parameter is $\Theta \approx 1.8$ at room temperature. In this 'strong entangler' limit, one finds

$$E_{N,\mathrm{out}} \overset{\xi \gg 1}{\rightarrow} -\frac{1}{2}\ln\left(1 - \frac{1}{\Theta} + \frac{1}{4}\frac{\xi^{-1}}{\Theta^3}\right), \tag{16}$$

from which it is evident that the magnitude of the negativity is being constrained solely by Θ, as depicted in figure 2. Although within the limits of our approximations, the output entanglement never totally vanishes, a soft, low-loss suspension is necessary to avoid diminution of the logarithmic negativity by thermal noise. To capture an appreciable fraction of the available entanglement, for a suspension with $\omega_m/2\pi \sim 1\,\mathrm{Hz}$ a quality factor $Q_m \sim 10^6$ is required. This is experimentally challenging but can be achieved, for example, in suspensions constructed of monolithic fused silica [38].

Finally, we observe that homodyne detection of both output optical fields provides a way to measure the covariance of any pair of quadratures, and hence to recover any element of the covariance matrix, permitting the entanglement borne by these fields to be quantified in an experimental setting. Such techniques have been demonstrated on entangled light produced by optical parametric oscillator systems [39, 40].

5. Concluding remarks

We have evaluated the capabilities of a ponderomotive entangler in a novel parameter regime that we believe is experimentally achievable. A singular feature of the system under consideration is the production of entanglement by gram-scale mechanical objects, while immersed in a room temperature environment. In addition, the produced entanglement can link

optical fields of widely separated frequencies, yielding a resource that may find applications in metrology [41]. Notable attributes of the apparatus that should allow observation of this entanglement include differential mode noise cancellation in the Fabry–Perot Michelson interferometer configuration, and the isolation from external forces supplied by the stiff optical trap. Construction and operation of this apparatus are underway at our laboratory.

Acknowledgments

We thank our colleagues at the LIGO Laboratory, especially Timothy Bodiya and Nicolas Smith, the AEI-Caltech-MIT MQM group, and Florian Marquardt of LMU, for helpful discussions. We gratefully acknowledge support from the National Science Foundation grants PHY-0107417 and PHY-0457264.

References

[1] Metzger C H and Karrai K 2004 *Nature* **432** 1002–5
[2] Naik A, Buu O, Lahaye M D, Armour A D, Clerk A A, Blencowe M P and Schwab K C 2006 *Nature* **443** 193–6
[3] Gigan S, Böhm H R, Paternostro M, Blaser F, Langer G, Hertzberg J B, Schwab K C, Bäuerle D, Aspelmeyer M and Zeilinger A 2006 *Nature* **444** 67–70
[4] Arcizet O, Cohadon P F, Briant T, Pinard M and Heidmann A 2006 *Nature* **444** 71–4
[5] Kleckner D and Bouwmeester D 2006 *Nature* **444** 75–8
[6] Schliesser A, Del'Haye P, Nooshi N, Vahala K J and Kippenberg T J 2006 *Phys. Rev. Lett.* **97** 243905
[7] Harris J G E, Zwickl B M and Jayich A M 2007 *Rev. Sci. Instrum.* **78** 013107
[8] Poggio M, Degen C L, Mamin H J and Rugar D 2007 *Phys. Rev. Lett.* **99** 017201
[9] Bose S, Jacobs K and Knight P L 1997 *Phys. Rev.* A **56** 4175–86
[10] Marshall W, Simon C, Penrose R and Bouwmeester D 2003 *Phys. Rev. Lett.* **91** 130401
[11] Mancini S, Giovannetti V, Vitali D and Tombesi P 2002 *Phys. Rev. Lett.* **88** 120401
[12] Zhang J, Peng K and Braunstein S L 2003 *Phys. Rev.* A **68** 013808
[13] Pinard M, Dantan A, Vitali D, Arcizet O, Briant T and Heidmann A 2005 *Europhys. Lett.* **72** 747–53
[14] Pirandola S, Vitali D, Tombesi P and Lloyd S 2006 *Phys. Rev. Lett.* **97** 150403
[15] Giovannetti V, Mancini S and Tombesi P 2001 *Europhys. Lett.* **54** 559–65
[16] Giannini S, Mancini S and Tombesi P 2003 *Quantum Inf. Comput.* **3** 265–79
[17] Armour A D, Blencowe M P and Schwab K C 2002 *Phys. Rev. Lett.* **88** 148301
[18] Ferreira A, Guerreiro A and Vedral V 2006 *Phys. Rev. Lett.* **96** 060407
[19] Vitali D, Gigan S, Ferreira A, Böhm H R, Tombesi P, Guerreiro A, Vedral V, Zeilinger A and Aspelmeyer M 2007 *Phys. Rev. Lett.* **98** 030405
[20] Paternostro M, Vitali D, Gigan S, Kim M S, Brukner C, Eisert J and Aspelmeyer M 2007 *Phys. Rev. Lett.* **99** 250401
[21] Müller-Ebhardt H, Rehbein H, Schnabel R, Danzmann K and Chen Y 2008 *Phys. Rev. Lett.* **100** 013601
[22] Braginsky V B and Vyatchanin S P 2002 *Phys. Lett.* A **293** 228–34
[23] Buonanno A and Chen Y 2002 *Phys. Rev.* D **65** 042001
[24] Corbitt T, Ottaway D, Innerhofer E, Pelc J and Mavalvala N 2006 *Phys. Rev.* A **74** 021802
[25] Sheard B S, Gray M B, Mow-Lowry C M, McClelland D E and Whitcomb S E 2004 *Phys. Rev.* A **69** 051801
[26] Miyakawa O *et al* 2006 *Phys. Rev.* D **74** 022001
[27] Corbitt T, Chen Y, Innerhofer E, Müller-Ebhardt H, Ottaway D, Rehbein H, Sigg D, Whitcomb S, Wipf C and Mavalvala N 2007 *Phys. Rev. Lett.* **98** 150802

[28] Corbitt T, Wipf C, Bodiya T, Ottaway D, Sigg D, Smith N, Whitcomb S and Mavalvala N 2007 *Phys. Rev. Lett.* **99** 160801
[29] Ou Z Y, Pereira S F, Kimble H J and Peng K C 1992 *Phys. Rev. Lett.* **68** 3663–6
[30] Silberhorn C, Lam P K, Weiß O, König F, Korolkova N and Leuchs G 2001 *Phys. Rev. Lett.* **86** 4267–70
[31] Bowen W P, Schnabel R, Lam P K and Ralph T C 2003 *Phys. Rev. Lett.* **90** 043601
[32] Peres A 1996 *Phys. Rev. Lett.* **77** 1413–5
[33] Simon R 2000 *Phys. Rev. Lett.* **84** 2726–9
[34] Plenio M B 2005 *Phys. Rev. Lett.* **95** 090503
[35] Adesso G and Illuminati F 2007 *J. Phys. A: Math. Theor.* **40** 7821–80
[36] Gardiner C W and Zoller P 2004 *Quantum Noise: A Handbook of Markovian and Non-Markovian Quantum Stochastic Methods with Applications to Quantum Optics* (*Springer Series in Synergetics*) (Berlin: Springer)
[37] Corbitt T, Chen Y, Khalili F, Ottaway D, Vyatchanin S, Whitcomb S and Mavalvala N 2006 *Phys. Rev.* A **73** 023801
[38] Cagnoli G, Gammaitoni L, Hough J, Kovalik J, McIntosh S, Punturo M and Rowan S 2000 *Phys. Rev. Lett.* **85** 2442–5
[39] Laurat J, Keller G, Oliveira-Huguenin J A, Fabre C, Coudreau T, Serafini A, Adesso G and Illuminati F 2005 *J. Opt. B: Quantum Semiclass. Opt.* **7** S577
[40] DiGuglielmo J, Hage B, Franzen A, Fiurášek J and Schnabel R 2007 *Phys. Rev.* A **76** 012323
[41] Grosse N B, Assad S, Mehmet M, Schnabel R, Symul T and Lam P K 2008 arXiv:0803.3784 [hep-th]